

Novel TOPP descriptors in 3D-QSAR analysis of apoptosis inducing 4-aryl-4H-chromenes: Comparison versus other 2D- and 3D-descriptors

Simone Sciabola,^{a,*} Emanuele Carosati,^a Lourdes Cucurull-Sanchez,^b
Massimo Baroni^c and Raimund Mannhold^{d,*}

^aLaboratory for Chemometrics and Cheminformatics, Chemistry Department, University of Perugia, Via Elce di Sotto, 10, I-06123 Perugia, Italy

^bPfizer Global Research and Development, Sandwich Laboratories, Sandwich, Kent, CT13 9NJ, UK

^cMolecular Discovery Ltd, 215 Marsh Road, HA5 5NE, Pinner, Middlesex, UK

^dMolecular Drug Research Group, Bldg. 22.03, Heinrich-Heine-Universität, Universitätsstrasse 1, 40225 Düsseldorf, Germany

Received 13 March 2007; revised 19 June 2007; accepted 26 June 2007

Available online 30 June 2007

Abstract—Novel 3D-descriptors using Triplets Of Pharmacophoric Points (TOPP) were evaluated in QSAR-studies on 80 apoptosis-inducing 4-aryl-4H-chromenes. A predictive QSAR model was obtained using PLS, confirmed by means of internal and external validations. Performance of the TOPP approach was compared with that of other 2D- and 3D-descriptors; statistical analysis indicates that TOPP descriptors perform best. A ranking of TOPP > GRIND > BCI 4096 = ECFP > FCFP > GRID-GOLPE >> DRAGON >> MDL 166 was achieved. Finally, in a ‘consensus’ analysis predictions obtained using the single methods were compared with an average approach using six out of eight methods. The use of the average is statistically superior to the single methods. Beyond it, the use of several methods can help to easily investigate the presence/absence of outliers according to the ‘consensus’ of the predicted values: agreement among all the methods indicates a precise prediction, whereas large differences between predicted values (for the same compounds by different methods) would demand caution when using such predictions.

© 2007 Elsevier Ltd. All rights reserved.

1. Introduction

The introduction of combinatorial chemistry and high throughput screening (HTS) in drug research yielded collections of large compound libraries with measured biological activities. When this highly valuable source of database information is properly manipulated with computer-assisted methods, it can aid to simplify the process of lead finding or of property-based design within a series of homologues. In the first case, molecular modelling approaches help to evaluate the molecular similarity/diversity within the database molecules. In the second case, modelling can contribute to optimise pharmacological or pharmacokinetic properties via QSAR models.

The success of such studies depends on the choice of an appropriate molecular characterization, producing a set of informative descriptors. Suitable characterizations must be, first of all, relevant to the properties to be studied. An excellent overview of many molecular descriptors is compiled by Todeschini and Consonni,¹ whereas suitability of molecular descriptors for database mining was analysed by Cruciani et al.² Classically, structural descriptors were derived from global molecular and physicochemical properties such as lipophilicity, electrostatics, steric shape and bulk. The main advantage is their fast computation, whereas a disadvantage is their lack of completeness and accuracy, at least in some cases.

Two-dimensional (2D) fragment-based descriptors are derived from substructure search systems. Most frequently used in drug research are structural keys and hashed fingerprints. The former make use of a predefined fragment dictionary and record the presence or absence of a number of small generic

Keywords: QSAR; Pharmacophores; Cell apoptosis; 2D-descriptors; 3D-descriptors.

* Corresponding authors. Tel.: +39 075 5855550; fax: +39 075 45646 (S.S.); tel.: +49 211 8112759; fax: +49 211 8111374 (R.M.); e-mail addresses: simone@chemiome.chm.unipg.it; mannhold@uni-duesseldorf.de

or specific fragments, whereas hashed fingerprints allow to reduce the length of the bitstring. In fact, a ‘molecular fingerprint’ is a binary bitstring of 1’s (for the presence) and 0’s (for the absence) of specific fragments and the use of hash functions allows to break the fingerprint into smaller strings, easier to handle. As for the structural descriptors, the main advantage of the 2D-descriptors is the speed of their calculation; the main drawback are difficulties in interpretation.

Among three-dimensional (3D)-descriptors, the GRID-based deserve particular mentioning. For their determination a molecule is placed in a box and for an orthogonal grid of points the interaction energy values between this molecule and a small probe molecule, such as water, are calculated. The GRID fields thus obtained, named Molecular Interaction Fields (MIF), characterize, for example, molecular shape, charge distribution and hydrophobicity. Development and successful application of GRID-based 3D-descriptors was recently summarized by Cruciani.³

In case of databases of several thousands of compounds, calculation time was always the bottleneck for using 3D-descriptors including those based on GRID. A novel member of the GRID-family overcomes this problem: the approach that uses Triplets Of Pharmacophoric Points (TOPP).⁴

In fact, the recently introduced TOPP descriptors⁴ lie between the two classes, 2D and 3D: they use the 3D-molecular structure and the parameterisation of the GRID force field but they resemble 2D-descriptors concerning speed and fingerprint style.

The aim of this study was to apply the novel TOPP-descriptors in a QSAR-study and to compare their performance with that of other 2D- and 3D-descriptors. A set of 4-aryl-4*H*-chromenes,^{5,6} exhibiting apoptosis-inducing potencies, served as database for such a case study.

Apoptosis is the normal process of cellular suicide that proceeds with specific biochemical and cytological features, including nuclear condensation and fragmentation. Apoptosis enables organisms to control their cell numbers and to eliminate unneeded cells.⁷ The correct balance between apoptosis and inhibition of apoptosis is important in preserving tissue homeostasis and organ morphogenesis.⁸ Aberrations of this process underlie some pathological conditions. Thereby, the biological interest in this field is steadily increasing, since many cancer cells exhibit abnormal inhibition of apoptosis⁹ while excessive apoptosis is implicated, for example, in Alzheimer’s disease.¹⁰

The discovery and development of apoptosis inducers are of prime current interest, and QSAR models can aid in specifying sound pharmacophoric considerations.

2. Dataset and methodology

2.1. Dataset

The dataset comprises 80 apoptosis-inducing 4-aryl-4*H*-chromenes; structural modifications mainly refer to substitution in 4-position and to substitution of the benzene part of the chromene ring. For this QSAR study the dataset was split into a training and a test set of 62 and 18 molecules, respectively. Their structures are listed in [Tables 1 and 2](#) according to the original articles;^{5,6} shaded structures represent members of the test set. The ‘Most Descriptive Compound’ (MDC) option, available in GOLPE,^{11,12} was used to automatically select a balanced and chemically diverse test set. The MDC criterion privileges a selection scheme that weights the compounds according to their population density.¹³

2.2. Biological data

Apoptosis-inducing potency was quantified by Kemnitzer et al.^{5,6} using a cell-based HTS assay in HL60 B-cell promyelotic leukaemia cancer cells. Potencies are listed in [Tables 1 and 2](#) in reciprocal logarithmic form ($\log 1/C$) for micromolar apoptosis induction. The spanned space of biological activity covers nearly 3 log units ranging from 7.96 for compound **32** to 5.14 for compound **39**.

2.3. 2D molecular descriptors

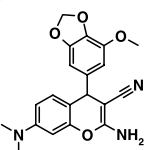
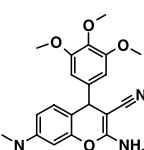
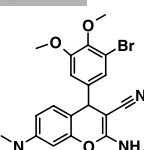
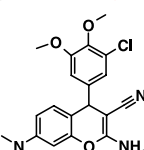
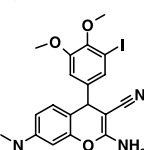
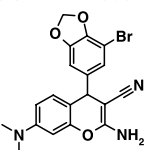
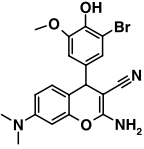
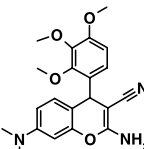
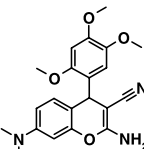
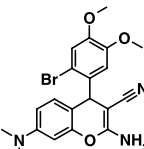
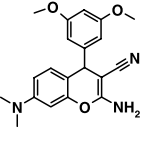
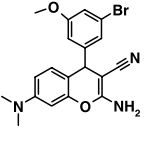
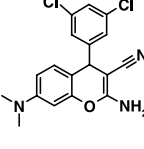
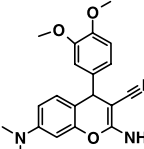
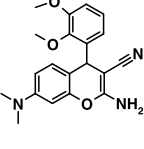
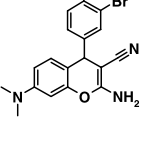
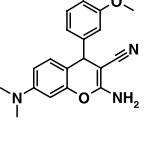
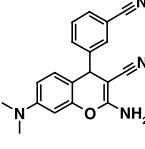
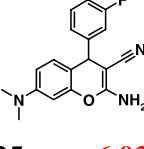
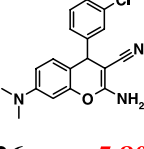
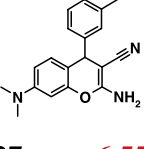
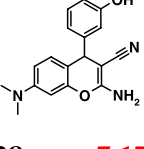
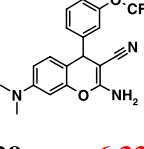
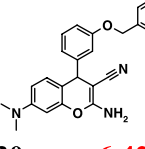
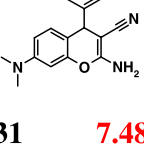
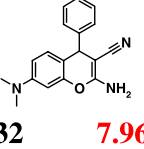
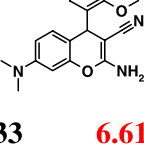
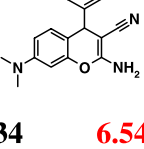
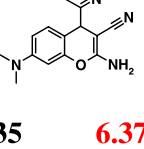
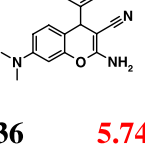
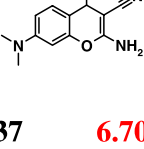
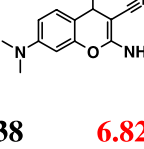
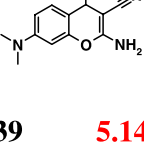
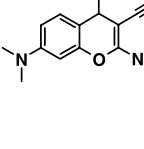
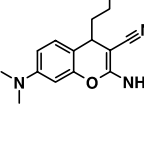
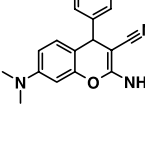
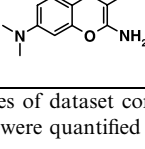
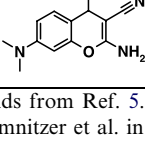
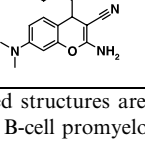
SD files were derived from SMILES notations and used as input for 2D-descriptors. MDL public keys, BCI fingerprints, ECFP and FCFP fingerprints were applied as 2D-descriptors in this study.

2.3.1. MDL public keys. MDL keys are used in QSAR, data-mining and virtual screening for substructure searching as well as for structure comparison. For these purposes, each molecule is regarded as a binary bitstring of 1’s and 0’s. A set of 166 keys, small topological substructure fragments, is used in tandem with a 960 key set which includes algorithmically generated, more abstract atom-pair descriptors. As many other 2D methods, the stereochemistry is not included in either set.^{14,15}

2.3.2. BCI fingerprints. BCI structural fingerprints of a molecule are based on the presence/absence of 2D structural features, listed in a predefined fragment dictionary. Six different families of fragments are available: augmented atoms, atom/bond sequences, atom pairs, ring composition fragments, ring fusion fragments and ring ortho fragments.¹⁶ A set of 4016 descriptors was used in this study.

2.3.3. ECFP and FCFP fingerprints. Pipeline Pilot from Scitec¹⁷ provides descriptors via following fragmentation scheme: each atom is represented by a string of extended connectivity values, calculated using a modified Morgan Algorithm (originally used in isomorphism issues¹⁸). Two different circular substructure descriptors were used in this study: Extended Connectivity Fingerprints (ECFPs) and Functional Connectivity

Table 1. Dataset structures I

01	7.14	02	7.35	03	7.72	04	7.74	105	7.74	06	6.61
											
07	7.39	08	5.50	09	5.75	10	5.58	11	7.64	12	7.51
											
13	7.12	14	6.60	15	5.99	16	7.19	17	7.19	18	7.20
											
19	7.09	20	6.95	21	6.87	22	6.57	23	6.35	24	5.60
											
25	6.93	26	5.80	27	6.55	28	7.17	29	6.33	30	6.42
											
31	7.48	32	7.96	33	6.61	34	6.54	35	6.37	36	5.74
											
37	6.70	38	6.82	39	5.14						
											

Structures of dataset compounds from Ref. 5. Shaded structures are members of the test set, the reported $\log 1/C$ values for apoptosis-inducing potency were quantified by Kemnitzer et al. in HL60 B-cell promyelotic leukaemia cancer cells.⁵

Fingerprints (FCFPs). The number of connections, the element type, the charge, and the mass determine the initial code assigned to an atom by ECFPs. Similarly, six generalised atom-types are used by FCFPs to assign the initial code: hydrogen-bond donor, hydrogen-bond acceptor, positively ionisable, negatively ionisable, aromatic and halogen. In both cases this code, combined with bond information and codes of its immediate neighbour atoms, is hashed to produce the next order code, which is mapped into an address space of size

$2E + 32$. The process is iterated until the required level of description has been achieved, in this case the standard ECFP₆ and FCFP₆. The Scitegic software represents a molecule by a list of integers, each describing a molecular feature and each in the range $-2E + 31$ to $2E + 31$. Calculation of these circular fingerprints is very fast and the features (size up to 4 billion) are not predefined in a limited fragment dictionary. These descriptors have been well tested in conjunction with the Laplacian-modified Bayesian analysis and have proved to be

Table 2. Dataset structures II

40	5.92	41	6.48	42	6.32	43	6.80	44	5.24	45	5.96
46	6.68	47	6.51	48	7.48	49	7.85	50	7.77	51	7.19
52	6.89	53	6.85	54	6.80	55	7.47	56	7.59	57	7.38
58	7.21	59	5.77	60	7.59	61	7.82	62	7.28	63	7.28
64	7.10	65	7.05	66	6.44	67	6.77	68	7.33	69	7.31
70	7.26	71	6.96	72	6.92	73	6.96	74	7.62	75	5.31
76	7.64	77	7.04	78	6.41	79	6.82	80	6.41		

Structures of dataset compounds from Ref. 6. Shaded structures are members of the test set, the reported log I/C values for apoptosis-inducing potency were quantified by Kemnitzer et al. in HL60 B-cell promyelotic leukaemia cancer cells.⁶

efficient in similarity-based virtual screening.^{19,20} In order to make this representation amenable for statistical analysis within GOLPE, the integers were hashed to a string of 1024 bits length.

2.4. 3D molecular descriptors

The three-dimensional structures of the compounds were obtained as follows. First, the 3D-coordinates of the 80

dataset compounds were converted from SMILES to 3D-coordinates with CONCORD.²¹ Then, the 3D-coordinates were minimized *in vacuo* with Sybyl,²² by applying the Powell method and using 1000 iterations. In order to guarantee a common alignment for all the compounds, compulsory for the GRID/GOLPE analysis, compound **03** served as template. The 4*H*-chromene scaffold was used for the superposition and as a guide to drive the roto-translation of all the compounds.

2.4.1. TOPP (Triplets of Pharmacophoric Points) descriptors. TOPP^{4,23} is a QSAR approach using 3-point pharmacophores as 3D-descriptors. The working protocol is represented in Figure 1. In the first step, the atoms of each molecule are classified by the GRID force field parametrization. In this way, atoms are described according to their charge and hydrogen bonding properties: DRY (hydrophobic), DONN (HBD, hydrogen bond donor), ACPT (HBA, hydrogen bond acceptor) and DNAC (both HBD and HBA). After the classification of the atoms an iterative procedure generates all possible combinations of three points with the four different atom types (DRY, DONN, ACPT and DNAC). Two different encoding modes exist: one approach is to store the presence/absence of each 3-point pharmacophore combination; the other approach is to count how many times each combination is present in the molecule. The calculations described above are performed for all the compounds and the resulting combinations of 3-point pharmacophores are the molecular descriptors. Descriptor coding such as ABC 07 08 07 indicates the atom types involved in a triplet (A = DRY, B = HB_DONOR, C = HB_ACCEPTOR) as well as the distances between them in Angstrom (dAB = 7 Å, dAC = 8 Å, dBC = 7 Å).²³ The final *X*-matrix, built up in a dynamic way so that no length of the bitstring is initially fixed, is submitted for statistical analysis.

2.4.2. GRIND descriptors. GRid-INdependent Descriptors GRIND²⁴ were generated using the software ALMOND.²⁵ The information contained in the Molecular Interaction Fields, computed by means of the GRID force field,^{26,27} is extracted to represent pharmacodynamic properties: in fact, GRIND descriptors represent the geometrical relationships between relevant MIF. The nodes showing favourable energies of probe-molecule interactions represent positions where groups of a receptor would interact favourably with the molecule. Hence, using different probes, one can obtain a set of such positions which define a virtual receptor site (VRS). The procedure for obtaining GRIND involves: (a) computing a set of MIF, (b) filtering the MIF to extract the most relevant nodes and (c) encoding the filtered MIF into the GRIND variables. The energy of the nodes and the distance between them guide the filtering procedure to extract the set of grid nodes (filtered MIF). Thereafter, the filtered nodes are encoded via MACC2 transform into few GRIND variables. Each variable is linked to a grid node-pair placed at a specific distance, and its value refers to the product of the energy values of the linked MIF, which represent attractive interactions between the probe and the molecule. GRIND

variables are organized in correlograms either representing node-pairs of the same field (auto-correlograms) or node-pairs of different fields (cross-correlograms). The following parameters were applied for calculations: 0.5 Å grid spacing, 120 nodes, 40% of weight assigned to the field, smoothing window width 0.6.

2.4.3. GRID/GOLPE descriptors.²⁸ Once all the compounds were superimposed, the GRID^{26,27} program was used to compute the Molecular Interaction Fields. GRID calculates the interaction energy between the molecule and a probe group which is moved through a regular grid of points around the target molecule. At each point, the interaction energy between the probe and the target molecule is calculated as the sum of Lennard–Jones potential (E_{LJ}), hydrogen-bond potential (E_{HB}), electrostatic contribution (E_{EL}) and an entropic term (S) necessary for the evaluation of the hydrophobic interaction:

$$E_{x,y,z} = \sum_{i=1}^N E_{LJ} + \sum_{i=1}^N E_{HB} + \sum_{i=1}^N E_{EL} + S \quad (1)$$

Different probes may be used to mimic specific interactions between the ligand and the receptor, since very often one probe is not enough to describe the interaction types of a given molecule. Therefore, a preliminary study was carried out with the probes DRY (Hydrophobic), C3 (Methyl), O (Carbonyl oxygen), N1 (Amide nitrogen) and OH (Phenolic hydroxyl) to investigate the effect of some different probes. A large cage (23 Å × 25 Å × 24 Å) was necessary to accommodate all the compounds, but the 13,800 ligand-probe energy measurements obtained for each compound were reduced to about 2969 after removal of variables with no variance.

The hydrophobic probe, DRY, and the phenolic hydroxyl probe, OH, were shown to be most effective. Therefore, we selected only these two probes for the GRID/GOLPE analysis.

2.4.4. DRAGON descriptors. DRAGON descriptors were developed by the Milano Chemometrics and QSAR Research Group²⁹ for application in QSAR and QSPR studies, as well as for similarity analysis and high-throughput screening of databases. DRAGON provides about 1500 molecular descriptors, divided into several logical blocks. In addition to the simplest counts of atom types, functional groups and fragments, there are topological and geometrical descriptors.¹ In our study, the whole set of DRAGON descriptors was used to build the *X*-matrix suitable for PLS analysis.

2.5. Statistical analysis

Partial Least Squares (PLS) analysis was performed within the software GOLPE.^{11,12} Scaling was applied according to the descriptors' type. The optimal dimensionality of the PLS model was chosen according to the results of cross validation. All computations were run on a Linux workstation (Pentium IV 3.4 GHz PC with 3 GB of main memory).

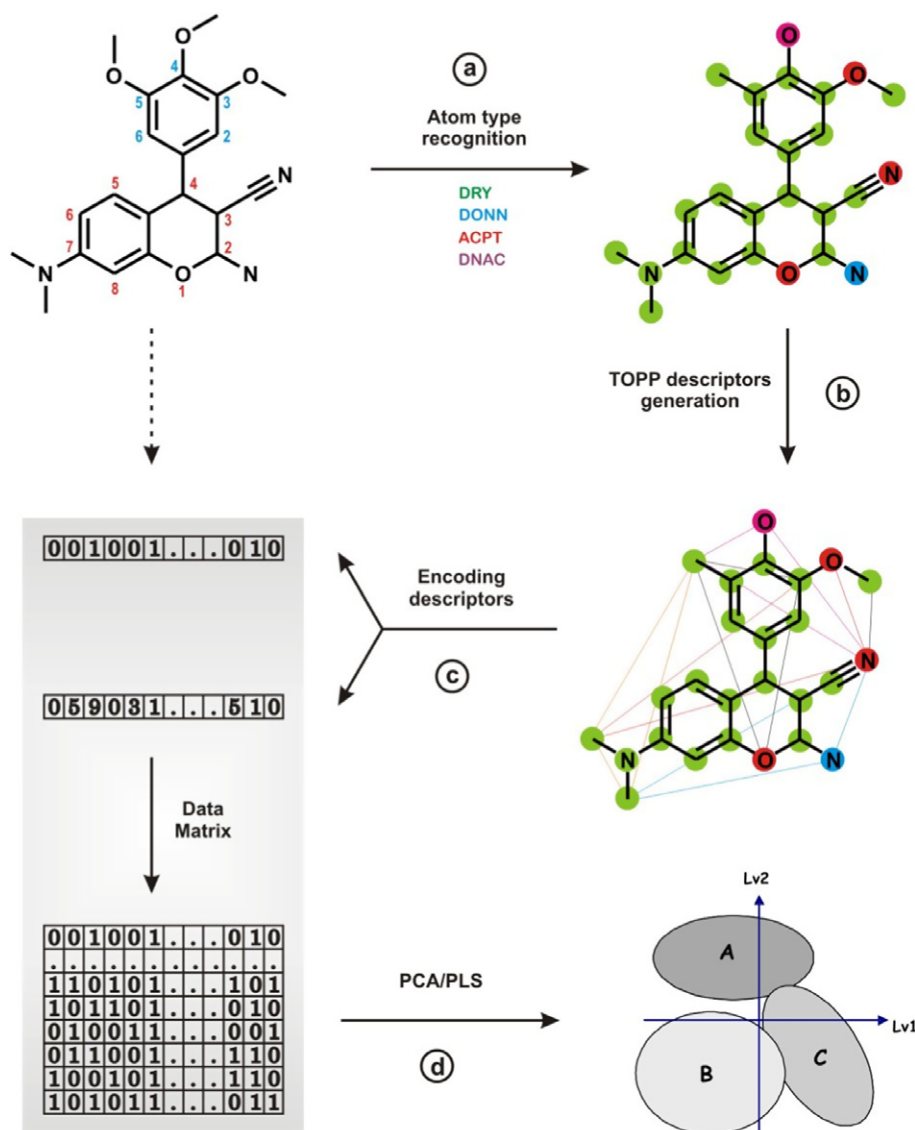


Figure 1. Working protocol in TOPP methodology. (a) The atoms of each molecule are classified by the GRID force field parameterization according to their charge and hydrogen bonding properties. (b) An iterative procedure generates all possible combinations of triplets with the four different atom types. (c) These triplets of pharmacophoric points are calculated for all database compounds and stored in a descriptors matrix. (d) Statistical analysis, that is, Principal Component Analysis (PCA) and Partial Least Square (PLS), can be applied.

3. Results and discussion

3.1. 3D-QSAR analysis using TOPP descriptors

With the 3-point pharmacophoric TOPP descriptors a starting PLS model was derived for the training set ($n = 62$); then, three fractional factorial design (FFD) runs (using default settings and the random group algorithm as cross-validation procedure) were used to select the variables for the X -space, which finally amounted to 375 TOPP descriptors. The resulting PLS model was optimal with five latent variables, explaining 91% of the variance for the apoptosis inducers in the training set, with a low standard deviation (0.21) of the error of calculation (SDEC). Internal validation was performed using five random groups: a q^2 value of 0.78 and a low standard deviation (0.32) of the error of

prediction (SDEP) were obtained. For external validation, the 18 test set compounds were projected and a SDEP of the same order of the internal validation (0.30) was achieved. The prediction of the test set is graphically represented in Figure 2. All compounds were satisfactorily predicted, showing how efficiently TOPP fingerprints can be used in QSAR studies.

Whenever QSAR models are part of lead optimisation projects, another important feature is to identify the variables with highest impact on biological activity; this information can help in the design of better compounds. When using PLS as regression tool, the coefficients profile plot helps to detect the most important variables; it is shown according to optimal model dimensionality in Figure 3. All variables (TOPP descriptors) are reported sequentially along the X -axis, where division bars were

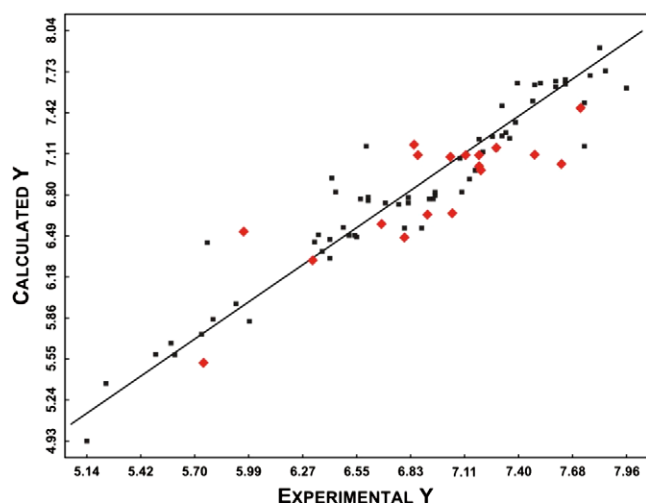


Figure 2. Calculated versus experimental values for the training set (62 compounds, black) and test set (18 compounds, red). The values reported are pEC_{50} obtained from Refs. 5 and 6.

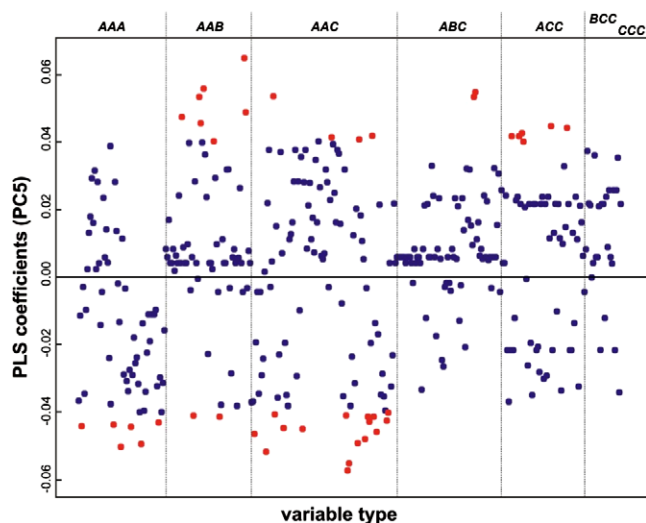


Figure 3. PLS coefficients plot for the TOPP model. All the descriptors are reported sequentially along the X-axis, and each division corresponds to a particular class of triplets. Red circles indicate those triplets that contribute most to explain the variance in biological activity, that is, they discriminate weak from potent compounds.

added to easily recognise variables corresponding to a particular class of triplets. It is noteworthy that the amount of active variables differs block by block; this is dataset-dependent and in our case there is a prevalence of DRY and ACPT atoms.

Variables with the largest coefficients contribute most to explain the variance in biological activity: they are represented with red circles. The cut-off value was arbitrarily set to ± 0.04 in order to include the variables that strongly discriminate weak from potent compounds. As indicated in the plot, these are the following few groups of variables: triplets AAA (DRY-DRY-DRY), ABC (DRY-HB_DONOR-HB_ACCEPTOR) and ACC (DRY-HB_ACCEPTOR-HB_ACCEPTOR). Triplets of the AAA type show high negative PLS coefficients; therefore they prevalently characterize inactive compounds. On the other hand, pharmacophoric triplets of the ABC and ACC type show large positive coefficients and thus they are important for classifying potent compounds. Together with the aforementioned types, two other triplet classes profoundly influence the biological behaviour of the training set compounds: AAB (DRY-DRY-HB_DONOR) and AAC (DRY-DRY-HB_ACCEPTOR). Unlike the others, AAB and AAC show both highly negative and positive coefficients; this indicates that their importance is related to the critical arrangement of distances they can assume in 3D, more than just the presence or absence of a particular combination of chemical features. The data in Table 3 underline such considerations. It is shown, whether a given 3-point interaction (the most relevant ones) is present or absent within two weak (**08**, **24**) and two potent (**32**, **49**) apoptosis inducers. Positive coefficients, highly indicative of potent compounds, prevail in potent inducers while the opposite is found for negative coefficients.

Once the highly relevant triplets are statistically defined, their graphical display within the original molecular structures allows to identify the chemical features favouring strong apoptosis induction. Moreover, it is possible to highlight molecular features inversely related to the biological activity, features that should be absent in a given compound in order to avoid weak apoptosis induction.

A putative pharmacophore can be hypothesized and linked to the SAR at 4-position of 4-aryl-4H-chromenes via grouping the most relevant variables (i.e., those with the highest positive PLS coefficients) for some potent compounds; they basically comprise the triplet types AAC, ABC, and ACC. For compounds **32** (Fig. 4a) and **49** (Fig. 5), these common features (AAC 07 08 07, AAC 09 08 06, ABC 07 07 04, ACC 04 02 06) suggest the importance of substitutions in the 3-(5-) position in both the phenyl and the pyridyl ring. Figure 4b

Table 3. Relevant triplets analysed in potent and weak compounds

		Positive coefficients					Negative coefficients				
		AAB 06 07 03	AAC 07 08 07	AAC 09 08 06	ABC 07 07 04	ACC 04 02 06	AAA 10 08 01	AAC 01 07 07	AAC 02 05 05	AAC 04 03 01	AAC 08 06 04
Potent	32	1	1	0	1	1	0	1	0	0	0
	49	1	1	1	1	1	0	0	0	0	0
Weak	08	0	0	1	0	0	0	1	1	1	0
	24	0	0	0	0	1	1	1	1	0	1

'1' and '0' denote presence or absence of the corresponding 3-point interaction.

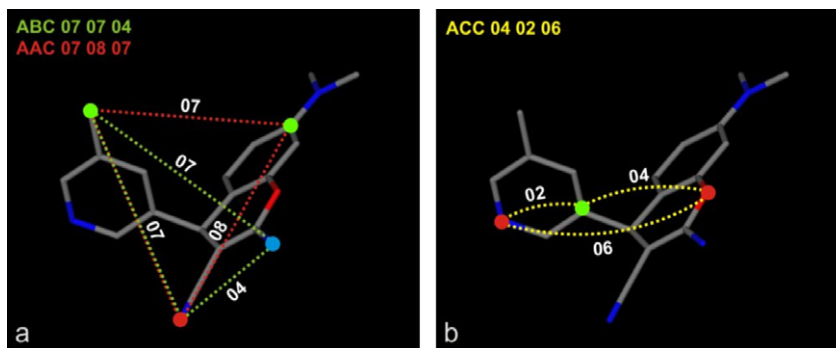


Figure 4. For the potent molecule **32** favourable triplet arrangements are shown. (a) The importance of substitution at 5-position is documented via the triplets ABC 07 07 04 and AAC 07 08 07. (b) The triplet ACC 04 02 06 expresses the importance of the nitrogen position in the pyridyl group.

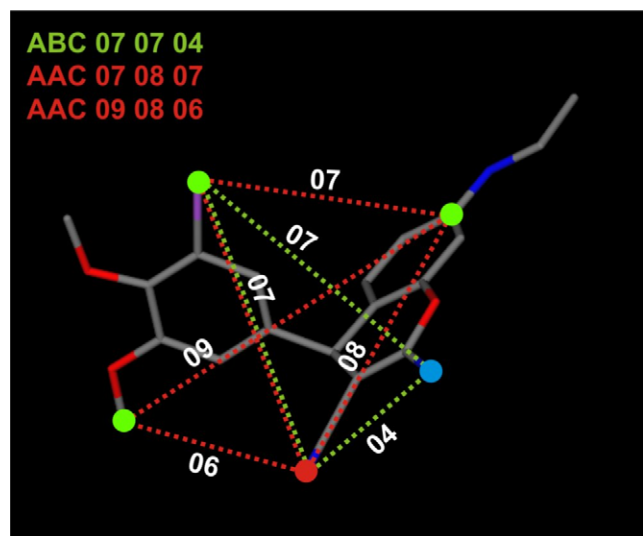


Figure 5. For the potent molecule **49** favourable triplet arrangements are shown comprising ABC 07 07 04, AAC 07 08 07, and AAC 09 08 06.

additionally shows the importance of the nitrogen position in the pyridyl group, confirming that in the pyridyl series it is important to have the nitrogen in 3-position with a substitution at 5-position.

Figure 6 shows variables with highly negative PLS coefficients (AAA 10 08 01, AAC 01 07 07, AAC 04 03 01, AAC 08 06 04), which are only present in weak inducers such as **08** and **24**. These variables define substitutions in the 4-phenyl ring that counteract apoptosis induction. Indeed, a 2-methoxy group renders **08** (Fig. 6a) >40-fold less active than the 3,4,5-trimethoxy analogue **02**, suggesting that there might be a space-limited pocket around the 2-position, or due to steric effect, the 2-methoxy group forces the phenyl ring into an unfavourable position.⁵ Same steric/size-limited pocket considerations hold for the 3-position, for example, in compound **24** (Fig. 6b), where replacing 3-methoxy by 3-benzyloxy leads to a >40-fold decrease of potency compared to **17**, as highlighted by highly negative coefficients for triplets AAA 10 08 01 and AAC 08 06 04.

Variable AAC 08 06 04 also allows interpreting the SAR of chromene scaffold-varied compounds from Ref. 6, shown in Table 2. Triplet AAC 08 06 04 in **45** corresponds to a triangle made by the chromene oxygen, the cyano carbon and the 6-methyl group (Fig. 7). Given its negative coefficient, the presence of this triplet contributes to decrease the apoptosis inducing potency of **45**, as agrees with previous reports^{5,6} that removal of 6-methyl can be determinant for retaining activity.

Analysis of the relevant TOPP variables did not provide further evidence related to the SAR at the chromene scaffold. Indeed, our model was not able to highlight the effect of substitution at 7–8-position, found to be

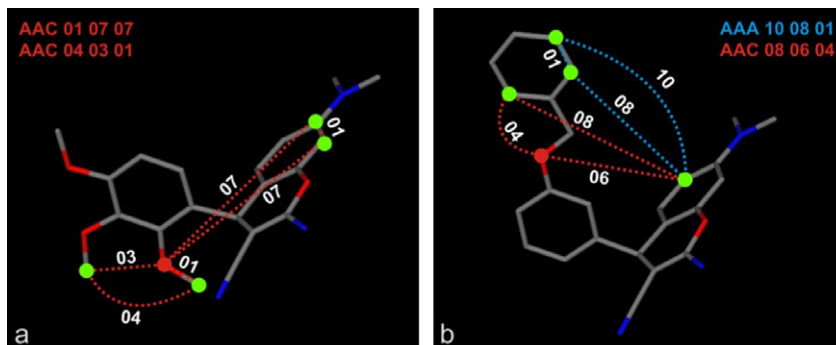


Figure 6. Unfavourable triplet arrangements for the molecules **08** (a) and **24** (b). Variables with highly negative PLS coefficients such as AAA 10 08 01, AAC 01 07 07, AAC 04 03 01 and AAC 08 06 04 are present in weak inducers such as **08** and **24**.

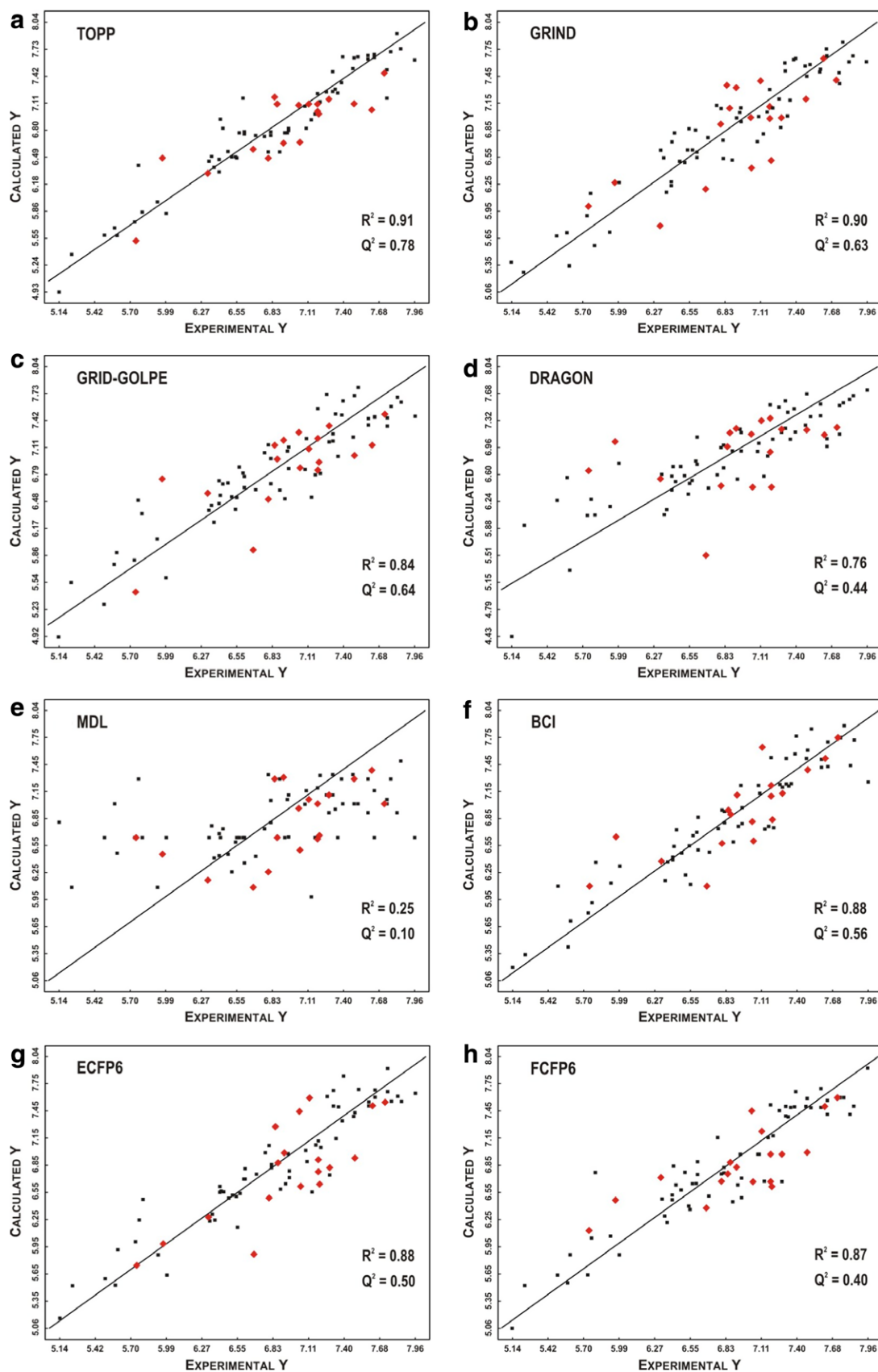


Figure 8. PLS scatter plots corresponding to the eight models; the corresponding statistical values are reported for each method.

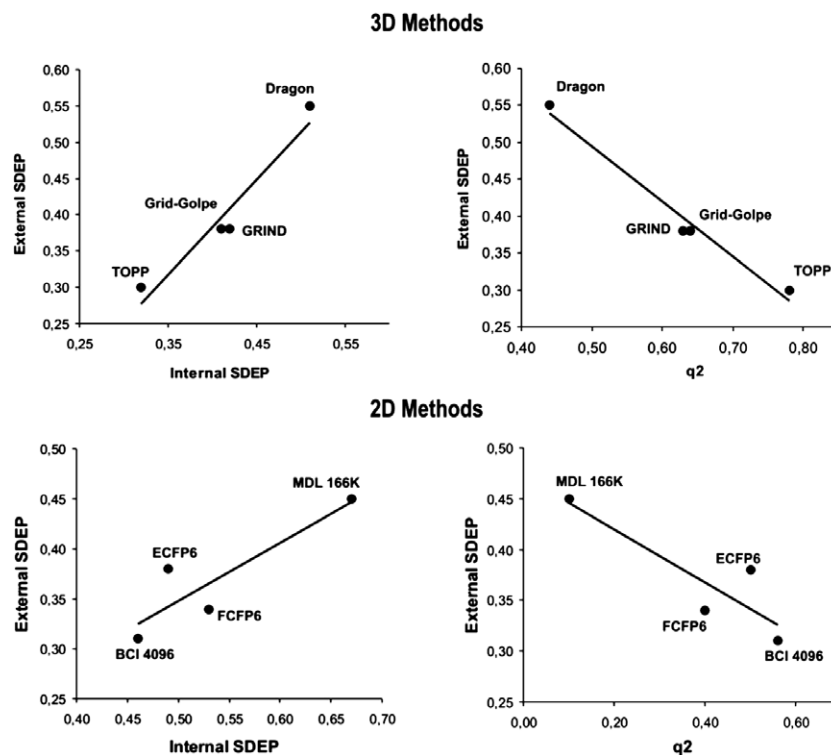


Figure 9. Trends related to different validations: internal and external validation are in agreement for the apoptosis dataset when analysing different 2D/3D-descriptors. The regression plots show good correlation when comparing both External versus Internal Standard Deviation of Errors of the Predictions and External SDEP versus q^2 values.

Circular substructure fingerprints ECFP₆ and FCFP₆, instead, seem to behave more stably from this point of view, giving reasonable statistical results independent from dataset composition. The same considerations hold for TOPP and GRIND, the former exhibiting best performance as QSAR descriptor both in this and the previously published study.²³

As shown in Figure 9, good correlation can be found when comparing the two different validation methodologies for 3D-and 2D-QSAR models, confirming the usefulness of such an internal validation tool in all cases where a limited dataset size does not allow a rigorous check of the real predictive power of the generated model via external validation.

The external validation analysis again confirmed TOPP as appropriate 3D-descriptors for QSAR analysis given the lowest SDEP (0.30) obtained for the 18 test set compounds. GRIND, GRID/GOLPE, BCI and Pipeline Pilot fingerprints also performed very well, having a SDEP value less than 0.40 and outperforming the remaining MDL and DRAGON approaches.

3.3. Average model versus single models

In pharmaceutical companies, a main goal of molecular modelling techniques is saving time and money, that is, focusing synthesis and biological tests only on promising molecules. This goal demands the availability of highly precise prediction tools. Therefore, we finally perform a ‘consensus’ analysis of the predictions obtained using

different methods and present an average approach using six out of eight methods to predict the apoptosis-inducing potency. DRAGON and MDL were excluded due to limited performance.

The results, reported in Figures 10 and 11, were intriguing: the use of the average is statistically superior to the single methods. In Figure 10 we compare the predictions of each method with the average of all predictions (for the same compounds), using the squared differences between experimental and predicted values. In case of better performances (lower differences) obtained with the average, the corresponding cell in the table is coloured in green. Vice versa, better performances obtained with a single method correspond to red colouring.

compd ID	TOPP	GRIND	GRID/GOLPE	BCI	ECFP	FCFP
03	-	-	-	+	+	+
09	-	-	-	-	+	-
13	+	+	+	-	-	+
16	+	-	+	+	-	-
17	+	+	-	+	-	-
18	+	-	+	+	-	-
21	-	-	-	+	+	+
42	+	-	-	-	-	-
43	-	+	-	-	-	+
45	-	+	-	-	+	-
46	+	+	-	-	-	+
48	+	+	-	+	-	-
53	-	-	-	+	-	+
63	+	-	+	+	-	-
65	-	-	+	-	-	+
72	-	-	-	+	+	-
74	-	+	-	+	+	+
77	+	+	-	-	-	-

Figure 10. Comparison of the predictions obtained with different models with the values obtained from the average.

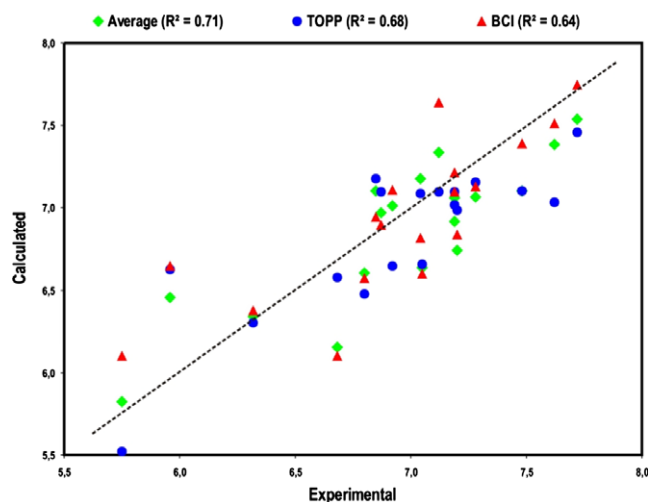


Figure 11. Calculated versus experimental values for the test set compounds obtained with TOPP (blue), BCI (red) and with the average (green).

Analysing Figure 10 by row (compound) indicates the average to generally overcome the single methods, analysing by column (method) shows that only BCI and TOPP perform at least as well as the average. The values predicted with TOPP, BCI and the average are presented together in Figure 11, where it is shown how the r^2 on the external set obtained doing the average is the highest (0.71), as well as the SDEP is the lowest (0.28).

Beyond it, the use of several methods can help to easily investigate the presence/absence of outliers according to the ‘consensus’ of the predicted values: agreement among all the methods indicates a precise prediction, whereas large differences between predicted values (for the same compounds by different methods) would demand caution when using such predictions.

4. Conclusion

The TOPP approach is a novel member in the family of GRID-based 3D-descriptors, although it does not refer directly to the interaction fields but uses the GRID atomic parameterization. In former papers, its successful application to CYP2D6 metabolic stability²³ and virtual screening³⁰ has been described. In such cases the method was applied to heterogeneous datasets comprising molecules with very diverse scaffolds. However, its performance for homogeneous datasets comprising molecules with the same scaffold—a frequent situation in QSAR studies—is missing yet.

Here, we present one of the first applications of TOPP descriptors and PLS analysis to QSAR studies on a dataset of 80 apoptosis-inducing 4-aryl-4H-chromenes.

Then, the performance of the TOPP approach was compared with that of other 2D-(MDL keys, BCI, ECFP

and FCFP fingerprints) and 3D-descriptors (GRIND, GRID/GOLPE, DRAGON); statistical criteria indicated that TOPP descriptors performed best.

Finally, predictions from the single methods were compared with an average approach using six out of eight methods indicating better results for the average approach.

Supplementary data

Supplementary data associated with this article can be found, in the online version, at [doi:10.1016/j.bmc.2007.06.051](https://doi.org/10.1016/j.bmc.2007.06.051).

References and notes

- Todeschini, R.; Consonni, V. *Handbook of Molecular Descriptors*. In *Methods and Principles in Medicinal Chemistry*; Mannhold, R., Kubinyi, H., Timmerman, H., Eds.; Wiley-VCH, 2000; Vol. 11.
- Cruciani, G.; Pastor, M.; Mannhold, R. *J. Med. Chem.* **2002**, *45*, 2685–2694.
- Cruciani, G. *Molecular Interaction Fields*. In *Methods and Principles in Medicinal Chemistry*; Mannhold, R., Kubinyi, H., Folkers, G. Eds.; Wiley-VCH; 2006; Vol. 27.
- Perruccio, F.; Mason, J.; Sciabola, S.; Baroni, M. FLAP: 4 point pharmacophore fingerprints from GRID. In *Molecular Interaction Fields in Drug Discovery*. In *Methods and Principles in Medicinal Chemistry*; Cruciani, G., Ed.; Wiley-VCH: Weinheim, 2005; Vol. 27, pp 83–102.
- Kemnitzer, W.; Kasibhatla, S.; Jiang, S.; Zhang, H.; Wang, Y.; Zhao, J.; Jia, S.; Herich, J.; Labreque, D.; Storer, R.; Meerovitch, K.; Bouard, D.; Rej, R.; Denis, R.; Blais, C.; Lamothe, S.; Attardo, G.; Gourdeau, H.; Tseng, B.; Drewe, J.; Cai, S. X. *J. Med. Chem.* **2004**, *47*, 6299.
- Kemnitzer, W.; Kasibhatla, S.; Jiang, S.; Zhang, H.; Zhao, J.; Jia, S.; Xu, L.; Crogan-Grundy, C.; Denis, R.; Barriault, N.; Vaillancourt, L.; Charron, S.; Dodd, J.; Attardo, G.; Labreque, D.; Lamothe, S.; Gourdeau, H.; Tseng, B.; Drewe, J.; Cai, S. X. *Bioorg. Med. Chem. Lett.* **2005**, *15*, 4745–4751.
- O'Driscoll, L.; Linehan, R.; Clynes, M. *Curr. Cancer Drug Targets* **2003**, *3*, 131–152.
- Reed, J. C.; Tomaselli, K. J. *Curr. Opin. Biotechnol.* **2000**, *11*, 586–592.
- Reed, J. C. *J. Clin. Oncol.* **1999**, *17*, 2941–2953.
- (a) Thompson, C. B. *Science* **1995**, *267*, 1456–1462; (b) Robertson, G. S.; Crocker, S. J.; Nicholson, D. W.; Schulz, J. B. *Brain Pathol.* **2000**, *10*, 283–292.
- Baroni, M.; Costantino, G.; Cruciani, G.; Riganelli, D.; Valigi, R.; Clementi, S. *Quant. Struct.-Act. Relat.* **1993**, *12*, 9–20.
- Golpe 4.5.12; <http://www.miasrl.com>.
- Hudson, S. B.; Hyde, M. R.; Rahr, E.; Wood, J. *Quant. Struct.-Act. Relat.* **1996**, *15*, 285–289.
- Durant, J. L.; Leland, B. A.; Henry, D. R.; Nourse, J. G. *J. Chem. Inf. Comp. Sci.* **2002**, *42*, 1273–1280.
- McGregor, M. J.; Pallai, P. V. *J. Chem. Inf. Comp. Sci.* **1997**, *37*, 443–448.
- Barnard, J. M.; Downs, G. M. *J. Chem. Inf. Comp. Sci.* **1997**, *37*, 141–142.
- Scitegic Inc., 9665 Chesapeake Dr., Suite 401, San Diego, CA 92123, USA, PipeLine Pilot 4.5.2, 2005, version 4.5.2.
- Morgan, H. L. *J. Chem. Doc.* **1965**, *5*, 107–113.

19. Hert, J.; Willett, P.; Wilton, D. J.; Acklin, P.; Azzaoui, K.; Jacoby, E.; Schuffenhauer, A. *J. Chem. Inf. Comp. Sci.* **2004**, *44*, 1177–1185.
20. Rogers, D.; Brown, R. D.; Hahn, M. *J. Biomol. Screen* **2005**, *10*, 682–686.
21. *Concord 5.1.2*; Tripos Inc., 1699 South Hanley Road, St. Louis, MO 63144.
22. *SYBYL 7.0*; Tripos Inc., 1699 South Hanley Road, St. Louis, MO 63144.
23. Sciabola, S.; Morao, I.; De Groot, M. J. *J. Chem. Inf. Comp. Sci.* **2007**, *47*, 76–84.
24. Pastor, M.; Cruciani, G.; McLay, I.; Pickett, S.; Clementi, S. *J. Med. Chem.* **2000**, *43*, 3233–3243.
25. Almond, version 3.2, is distributed from Molecular Discovery Ltd, <http://www.moldiscovery.com>.
26. Goodford, P. J. *J. Med. Chem.* **1985**, *28*, 849–857.
27. Carosati, E.; Sciabola, S.; Cruciani, G. *J. Med. Chem.* **2004**, *47*, 5114–5125.
28. Cruciani, G.; Watson, K. A. *J. Med. Chem.* **1994**, *37*, 2589–2601.
29. Milano Chemometrics and QSAR Research Group, Department of Environmental Sciences, Milano, Italy, Dragon, 2002, version 2.1.
30. Carosati, E.; Mannhold, R.; Wahl, P.; Hansen, J. B.; Fremming, T.; Zamora, I.; Cianchetta, G.; Baroni, M. *J. Med. Chem.* **2007**, *50*, 2117–2126.